Gas Phase Reaction of Substituted Isoquinolines to Carboxylic Acids in Ion Trap and Triple Quadrupole Mass Spectrometers after Electrospray Ionization and Collision-Induced Dissociation

Mario Thevis,[a] Maxie Kohler,[a] Nils Schlörer,[b] and Wilhelm Schänzer[a]

[a] Center for Preventive Doping Research, Institute of Biochemistry, German Sport University Cologne, Cologne, Germany
[b] Institute of Organic Chemistry, University of Cologne, Cologne, Germany

Within the mass spectrometric study of bisubstituted isoquinolines that possess great potential as prolylhydroxylase inhibitor drug candidates (e.g., FG-2216), unusually favored gas-phase formations of carboxylic acids after collisional activation were observed. The protonated molecule of [(1-chloro-4-hydroxy-isoquinoline-3-carbonyl)-amino]-acetic acid was dissociated, yielding the 1-chloro-4-hydroxy-isoquinoline-3-carboxylic acid methyleneamide cation. Subsequent dissociation caused the nominal elimination of 11 u that resulted from the loss of HCN and concomitant addition of oxygen to the product ion, which formed the protonated 1-chloro-4-hydroxy-isoquinoline-3-carboxylic acid. The preference of this structure under mass spectrometric conditions was substantiated by tandem mass spectrometry analyses using the corresponding methyl ester (1-chloro-4-hydroxy-isoquinoline-3-carboxylic acid methyl ester) that eliminated methylene (−14 u) upon collisional activation. Moreover, the major product ion of 1-chloro-4-hydroxy-isoquinoline-3-carboxylic acid, which resulted from the loss of water in MS^3 experiments, restored the precursor ion structure by re-addition of H_2O. Evidences for these phenomena were obtained by chemical synthesis of proposed gas-phase intermediates, H/D exchange experiments, high-resolution/high accuracy mass spectrometry at MS^n level, and "ping-pong" analyses (MS^7, in which the precursor ion was dissociated and the respective product ion isolated to regenerate the precursor ion for repeated dissociation. Based on these results, dissociation pathways for [(1-chloro-4-hydroxy-isoquinoline-3-carbonyl)-amino]-acetic acid were suggested that can be further utilized for the characterization of structurally related compounds or metabolic products in clinical, forensic, or doping control analysis. (J Am Soc Mass Spectrom 2008, 19, 151–158) © 2008 American Society for Mass Spectrometry

Prolyl hydroxylases have been subject of various studies because of their importance in several biochemical pathways and, thus, related diseases in case of impaired activity. Proline hydroxylation was identified as a key factor in the biosynthesis and maturation of collagen [1, 2], which requires 4-hydroxylation of specific proline residues (in X-Pro-Gly motifs) to establish the characteristic triple-helical structure. However, during life-threatening fibrotic states, inappropriately large amounts of collagen are produced, and the inhibition of proline hydroxylation is desired to divert the collagen biosynthesis into a degradative pathway [3]. More recently, the catalytic role of prolyl hydroxylase isoforms in modifying conserved prolines of two oxygen-dependent degradation domains in the hypoxia-inducible factor (HIF)-1α was identified [4–6]. The members of the 2-oxoglutarate-dependent dioxygenase superfamily enable the hydroxylation of the proline residues 402 and 564 of HIF-1α and promote its degradation via ubiquitylation and subsequent proteasomal destruction [7–9]. As a consequence, the presence of HIF-1α in organisms is regulated in an oxygen-dependent manner, which represents the basis of cellular oxygen sensing [10–12] and, thus, the activity of hypoxic response genes that control angiogenic [13, 14] and erythropoietic processes [15–17].

Based on these findings and the involved molecular principles, numerous compounds were designed and tested regarding their properties to inhibit prolyl hydroxylase activities to counteract and correct symptoms of serious diseases. Derivatives of 2-oxoglutarate [18, 19], hydroxyanthraquinones [20], 5-acyl sulfonamides [21], dihydroxybenzoates [22], hydroxyquinolines [23], pyrazolopyridines [24], and many other compounds [25–28] were

Address reprint requests to Dr. Mario Thevis, Institute of Biochemistry, Center for Preventive Doping Research, German Sport University Cologne, Carl-Diem Weg 6, 50933 Cologne, Germany. E-mail: m.thevis@biochem.dshs-koeln.de

1044-0305/08/$32.00
doi:10.1016/j.jasms.2007.11.003

Published online November 9, 2007
Received October 1, 2007
Revised November 2, 2007
Accepted November 4, 2007

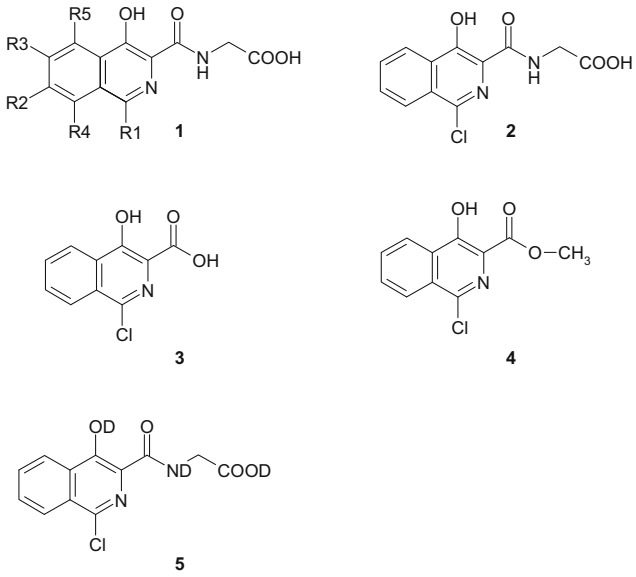

Scheme 1. Chemical structures of investigated: **1,** general structure of isoquinoline-3-carboxylamide-based prolylhydroxylase inhibitors, **2,** drug candidate (mol $wt_{monoisotopic}$ = 280), **3,** 1-chloro-4-hydroxy-isoquinoline-3-carboxylic acid (mol $wt_{monoisotopic}$ = 223), **4,** 1-chloro-4-hydroxy-isoquinoline-3-carboxylic acid methyl ester (mol $wt_{monoisotopic}$ = 237), and **5,** drug candidate **2** after H/D-exchange in D_2O/MeOD (mol $wt_{monoisotopic}$ = 283). R1-R5 represent various substituents, e.g., hydrogens, halogens, hydroxyl functions, alkyl, or alkyloxy residues, etc.

prepared and studied. One of the most promising class of candidates, which currently undergoes Phase II clinical trials [29], comprises an isoquinoline core with a 3-positioned carboxyl residue that was converted into its amide using glycine (Scheme **1**-1). Various studies proved the efficiency of the lead drug candidate FG-2216, an orally active compound, in stimulating erythropoiesis for the treatment of anemia [30, 31]. In the course of analytical assay development concerning model prolyl hydroxylase inhibitors (PHIs), the isoquinoline-derived PHI [(1-chloro-4-hydroxy-isoquinoline-3-carbonyl)-amino]-acetic acid was synthesized, and subsequently studied using electrospray ionization and high-resolution/high accuracy ion trap/orbitrap mass spectrometry. Diagnostic product ions characterizing the target analyte and related compounds were elucidated in MS^n experiments with in-time and in-space dissociation as well as comparison of ions formed under gas-phase conditions with chemically synthesized reference substances. The obtained results provided evidence for gas-phase reactions that include the addition of oxygen as well as water generating a favored ion with isoquinoline-3-carboxylic acid structure. The resulting data on the dissociation behavior of structural analogs shall support the identification of such compounds and/or metabolites in clinical, forensic, and doping control analysis.

Experimental

To allow method developments aiming at clinical, forensic, or preventive doping research, therapeutics in clinical studies or structural analogs that resemble physicochemical properties of future drug candidates are studied using informative and sensitive analytical tools such as mass spectrometry, which are applicable also to biological matrices.

Chemicals and Reagents

Phthalic anhydride (99%), methyl isocyanoacetate (97%), phosphorus oxychloride (99%), glycine methyl ester hydrochloride (99%), (benzotriazol-1-yloxy)tripyrrolidinophosphonium hexafluorophosphate (PyBOP, 98%), triethylamine (99%), *N*-ethyldiisopropylamine (98%), deuterium oxide (D_2O, 99.9%), and water-^{18}O (10%) were purchased from Sigma (Deisendorf, Germany). Silica gel 60 (70-230 mesh) and solvents (methanol, tetrahydrofurane, dichloromethane, and dimethylformamide, all analytical grade) were obtained from Merck (Darmstadt, Germany). Deionized water used for sample preparation and buffer solutions was of MilliQ grade.

Synthesis and Characterization of Model Compound

One model PHI, [(1-chloro-4-hydroxy-isoquinoline-3-carbonyl)-amino]-acetic acid (Scheme **1**-2) and related derivatives were synthesized as described elsewhere [32, 33]. Briefly, phthalic anhydride and methyl isocyanatoacetate were mixed to yield to 5-(2-carboxyphenyl)-4-methoxycarbonyl-1,3-oxazole, which was further condensed to methyl 4-hydroxy-1-oxo-1,2-dihydroisoquinoline-3-carboxylate, which is referred to as Compound **4** (Scheme **1**) that allowed the preparation of Compound **3** (Scheme **1**) after alkaline hydrolysis. Subsequent chlorination at C-1, amide formation at the 3-carboxyl function using glycine methyl ester, and alkaline hydrolysis gave rise to Compound **2**. After purification using flash chromatography (dichloromethane and silica gel), the pure reference compound was characterized by nuclear magnetic resonance spectroscopy (NMR) with ^1H, H,H-COSY, H,C HMQC, H,C HMBC, and DEPT experiments employing a Bruker DRX 500 MHz instrument (Bruker, Karlsruhe, Germany) equipped with a 5 mm inverse probe head (z-gradient coil). Approximately 10 mg of **2** was dissolved in deuterated dimethylsulfoxide, and spectra were recorded at room temperature. In addition, the elemental composition of the synthesized substance was determined using high-resolution/high accuracy mass spectrometry utilizing an LTQ Orbitrap (Thermo, Bremen, Germany) at a resolving power of 30,000 (FWHM).

Stock and Working Solutions

The stock solutions of the analytes was prepared in acetonitrile at 1 mg/mL and stored at 2 to 8 °C. Working solutions were prepared at 2 μg/mL using acetoni-

trile and water (1:1, vol:vol) acidified with 0.5% of formic acid.

Electrospray Ionization-Tandem Mass Spectrometry

ESI-MS(/MS) was performed on a LTQ Orbitrap (Thermo, Bremen, Germany) mass spectrometer. The instrument was operated in positive ionization mode and calibrated using the manufacturer's calibration mixture (containing caffeine, MRFA, and Ultramark that yield a total of seven reference masses). Mass accuracies < 2 ppm (calculated from 30 averaged spectra) were determined before and after the period of analysis of target compounds. Working solutions were introduced into the mass spectrometer using a syringe pump at a flow rate of 5 μL/min. The ionization voltage was 3.0 kV, the capillary temperature was set to 275 °C, and protonated precursor ions were isolated using a width of 1.4 Da. The protonated species were dissociated at normalized collision energies between 10 and 35 (arbitrary units). Damping gas in the linear ion trap was helium (purity grade 5.0), and gas supplied to the curved linear ion trap (CLT) was nitrogen obtained from a CMC nitrogen generator (CMC Instruments, Eschborn, Germany).

H/D-Exchange Experiments

To provide more detailed mass spectrometric information for product ion characterization and suggestion of dissociation pathways, hydrogen/deuterium-exchange was performed by dissolving 1 mg of Compound **2** in 1 mL of deuterated methanol (MeOD) and deuterium oxide (D_2O) (1:1, vol:vol). After incubation at room temperature for 10 min, the solution was diluted 1:50 in MeOD/D_2O (1:1, vol:vol) and introduced into the LTQ Orbitrap mass spectrometer via the syringe pump. Analyses were carried out under identical conditions as applied for Compound **2** without H/D-exchange.

Liquid Chromatography-Tandem Mass Spectrometry

Additional mass spectrometric studies were performed using an Agilent 1100 Series liquid chromatograph (Waldbronn, Germany) coupled to an Applied Biosystems API 4000 QTrap mass spectrometer (Darmstadt, Germany) with electrospray ionization to probe for differences in dissociation pathways using in-space instead of in-time tandem mass spectrometry and nitrogen as collision gas. The LC was equipped with a Macherey-Nagel Pyramid column (4.0 $\times$ 70 mm, 5 μm particle size), and the eluents used were 5 mM ammonium acetate containing 0.1% acetic acid (mobile phase A) and acetonitrile/methanol (1:1, vol:vol; mobile phase B). A gradient was employed starting at 0% B (1 min) increasing to 100% B within 6.5 min followed by re-equilibration at 0% B for 1.5 min. The flow rate was set to 800 μL/min. Nitrogen was employed as curtain and collision gas (5×10^{-3} Pa) delivered from a CMC nitrogen generator (CMC Instruments, Eschborn, Germany), and collision offset voltages or nozzle-skimmer dissociation settings were optimized for each experiment (vide infra).

Results and Discussion

Synthesis and Characterization of the Model PHI [(1-Chloro-4-Hydroxy-Isoquinoline-3-Carbonyl)-Amino]-Acetic Acid

The synthesis yielded the intended structure with an overall yield 8.6%, which provided sufficient amounts of pure analyte necessary for structure characterization and mass spectrometric studies. Compound **2** was characterized by NMR analyses: ^{1}H NMR (500 MHz, d_6-DMSO) δ: 8.35 (m, 1H, H-5), 7.99 (m, 1H, H-6), 7.99 (m, 1H, H-7), 8.35 (m, 1H, H-8), 4.05 (d, 2H, H-13); ^{13}C NMR (125 MHz, d_6-DMSO) δ: 139.1 (C-1), 120.9 (C-3), 155.0 (C-4), 123.5 (C-5), 132.2 (C-6), 132.2 (C-7), 126.6 (C-8), 130.0 (C-9), 129.0 (C-10), 169.3 (C-11), 41.35 (C-13), 171.1 (C-14).

Electrospray Ionization-tandem Mass Spectrometry

The CID behavior of the model target analyte **2** was studied employing high-resolution/high accuracy (tandem) mass spectrometry with a hybrid linear ion trap-orbitrap instrument. The characterization of dissociation pathways of new emerging therapeutics is of particular importance in clinical research as well as sports drug testing. Metabolite identification and characterization nowadays strongly relies on mass spectrometric results, which necessitate a comprehensive set of information to assign dissociation pathways to analyte structures in complex biological matrices such as blood or urine.

PHIs have been the subject of various recent studies [23, 24], and the product ion spectrum of **2** derived from the protonated molecule $[M + H]^+$ at *m/z* 281 is depicted in Figure 1a. Upon weak collisional activation (normalized collision energy = 15 arbitrary units, Xcalibur Software version 2.0; Thermo, San Jose, CA), the precursor ion consecutively eliminates water (−18 u) and carbon monoxide (−28 u) yielding the product ions at *m/z* 263 and 235, respectively. Moreover, a nominal loss of C_2H_3NO (−57 u) is observed generating the ion at *m/z* 224, which subsequently releases water (−18 u) to yield the product ion at *m/z* 206 (Table 1). By means of MS^3 and MS^4 experiments, it was demonstrated that the ion at *m/z* 235 gives rise to *m/z* 224 (Figure 1b). This corresponded to a nominal loss of 11 u that was attributed to the elimination of HCN (−27 u) concerted with an addition of oxygen (+16 u) according to high-resolution/high accuracy mass spectrometry results (Table 1). Due to this unusual behavior, various exper-

iments, including linear ion trap MS^n and in-space MS/MS, H/D-exchange, as well as synthesis and analysis of putative compounds generated in situ as gas-phase ions under CID conditions, were conducted to elucidate the mechanism underlying the observed dissociation behavior.

The influence of ion trapping on the phenomenon of the release of HCN and the simultaneous addition of oxygen to the ion at *m/z* 235 was evaluated using a triple-stage quadrupole tandem mass spectrometer (Applied Biosystems QTrap 4000, see above). Employing an elevated declustering potential of 100 V that induces a nozzle-skimmer dissociation of the protonated precursor ion to generate *m/z* 235, pseudo-MS^3 measurements were performed that yielded a highly comparable dissociation pattern as observed in ion trap/orbitrap analyses. The major product ions formed from *m/z* 235 using in-space CID were found at *m/z* 224 and *m/z* 206 (Figure 1c), which allowed the assumption that the rearrangement causing the loss of HCN and the addition of oxygen did not necessitate ion trapping conditions and was not dependent on resonant excitation of ions. Exchanging hydrogen by deuterium atoms in Compound **2** yielded the precursor ion at *m/z* 285 (Scheme **1**, 5) due to the incorporation of three deuterons plus one replacing the proton, which is added during the ionization process. The dissociation of the deuterated precursor ion $[M_{D3} + D]^+$ provided evidence for the loss of D_2O (−20 u) followed by the elimination of CO (−28) giving rise to product ion at *m/z* 237 that comprised two deuterium atoms (Table 1). Moreover, product ions at *m/z* 225 and 227 were detected, which proved the existence of two dissociation pathways and supposedly two different structures of product ions with identical elemental compositions in case of the unlabeled Compound **2**; i.e., the precursor ion of the deuterated Compound **5** eliminated isocyanatomethane containing one deuterium atom (CH_2DNCO, −58 u) to yield *m/z* 227, while MS^3 experiments using *m/z* 237 as the second precursor ion generated the product ion at *m/z* 225 that resulted from the loss of DCN accompanied by the uptake of one oxygen atom (Table 1). The source of the added oxygen, however, remained unclear. Based on these data, dissociation pathways for the protonated molecule of **2** were proposed as illustrated in Scheme **2**. Two parallel routes led to the product ion at *m/z* 224, which is assumed to be composed by two species. Route 1 is suggested to be initiated by the losses of water and carbon monoxide (a) that yielded the 1-chloro-4-hydroxy-isoquinoline-3-carboxylic acid methyleneamide cation at *m/z* 235 (Scheme **2**). The elimination of HCN (b) can form a highly reactive carbene that subsequently adds oxygen (c) to yield *m/z* 224. In contrast, route 2 is proposed to consist of an immediate release of isocyanatomethane (d) from the protonated molecule. Here, a rearrangement including hydrogen transfer from N-2 to the leaving group and migration of the terminal carboxyl function are suggested because only one deuterium atom was eliminated with the loss of CH_2DNCO in H/D-exchange experiments (vide supra).

Supporting information for the suggested structures of the product ions at *m/z* 235 and 224 were obtained by further dissociation as well as analyses of synthesized 1-chloro-4-hydroxy-isoquinoline-3-carboxylic acid (Scheme **1**-3) and its methyl ester (Scheme **1**-4). Besides abundant signals at *m/z* 224 and 206, the ion at *m/z* 235 (derived from Compound **2**) yielded a product ion at *m/z* 178 in MS^3 experiments (Figure 1b, Table 1). Its generation was assigned to the loss of N-methylene-formamide (CH_2NCHO, −57 u), which is possible after isomerization of *m/z* 235 with charge delocalization via a facile 1,2-elimination assuming the structure presented in Scheme **2** (e). The CID of the product ion at *m/z* 224 mainly yielded an ion resulting from the loss of water only (*m/z* 206) but also products resulting from the consecutive release of CO (*m/z* 196) and water (*m/z* 178) (Figure 1d). The analysis of synthesized 1-chloro-4-hydroxy-isoquinoline-3-carboxylic acid (Compound **3**), which represents the proposed structure of the product ion at *m/z* 224, demonstrated an identical dissociation behavior as the product ion derived from Compound **2**, which substantiated the postulated gas-phase ion structure (Figure 1e). Measuring the corresponding methyl ester of 1-chloro-4-hydroxy-isoquinoline-3-carboxylic acid (Compound **4**) under identical conditions gave rise to a product ion spectrum depicted in Figure 1f. The protonated molecule at *m/z* 238 generated an abundant signal upon collisional activation at *m/z* 224, which represented the free carboxylic acid and, thus, demonstrated the favored gas-phase ion structure of *m/z* 224 as the loss of methylene is rather seldom using ESI and CID.

Finally, the preferred generation of *m/z* 224 was further substantiated by isolation of its major product ion at *m/z* 206 (Scheme **2**). The isolation and storage of *m/z* 206 in the linear ion trap without excitation enabled the restoration of *m/z* 224 by the re-addition of water

Figure 1. ESI product ion spectra of (**a**) Compound **2**, LTQ-Orbitrap, collision energy = 15 arbitrary units; (**b**) Compound **2**, LTQ-Orbitrap, MS^3 experiment on *m/z* 281–235, collision energy = 17 arbitrary units; (**c**) Compound **2**, API 4000 QTrap, pseudo-MS^3 experiment on *m/z* 235, declustering potential = 100 V, collision offset voltage = 20 V; (**d**) Compound **2**, LTQ-Orbitrap, MS^3 experiment on *m/z* 281–224, collision energy = 25 arbitrary units; (**e**) Compound **3**, LTQ-Orbitrap, (1-chloro-4-hydroxy-isoquinoline-3-carboxylic acid), collision energy = 40 arbitrary units; and (**f**) Compound **4**, LTQ-Orbitrap, (1-chloro-4-hydroxy-isoquinoline-3-carboxylic acid methyl ester), collision energy = 17 arbitrary units.

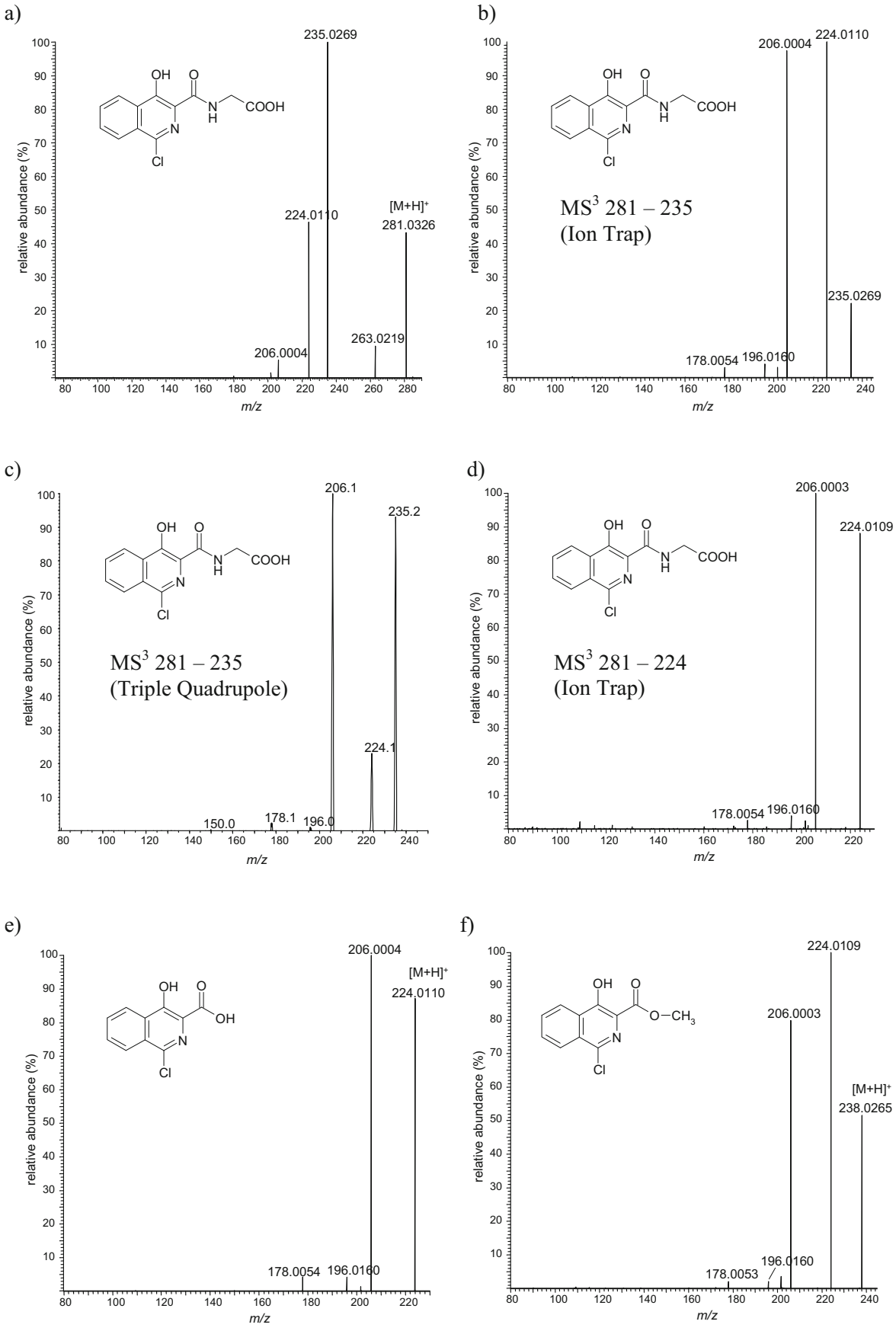
a)
235.0269
224.0110
[M+H]+
281.0326
263.0219
206.0004
b)
206.0004
224.0110
MS3 281 – 235
(Ion Trap)
235.0269
178.0054
196.0160
c)
206.1
235.2
MS3 281 – 235
(Triple Quadrupole)
224.1
150.0
178.1
196.0
d)
206.0003
224.0109
MS3 281 – 224
(Ion Trap)
178.0054
196.0160
e)
206.0004
[M+H]+
224.0110
178.0054
196.0160
f)
224.0109
206.0003
[M+H]+
238.0265
196.0160
178.0053
relative abundance (%)
m/z

Table 1. Elemental compositions of protonated molecules and resulting product ions using high resolution/high accuracy MS^n experiments

Compound	Precursor ion (*m/z*)			Elemental comp. (exp.)	Error (ppm)	Collision energy (arb. units)	Product ion (*m/z*)	Elemental comp. (exp.)	Error (ppm)	Cleaved species
	MS^2	MS^3	MS^4							
2	281.0326			$C_{12}H_{10}O_4N_2Cl$	0.7	15	263.0219	$C_{12}H_8O_3N_2Cl$	0.3	H_2O
							235.0269	$C_{11}H_8O_2N_2Cl$	0.1	H_2O, CO
							224.0110	$C_{10}H_7O_3NCl$	0.4	C_2H_3NO
							206.0004	$C_{10}H_5O_2NCl$	0.3	C_2H_3NO, H_2O
		263.0219		$C_{12}H_8O_3N_2Cl$	0.3	10	235.0269	$C_{11}H_8O_2N_2Cl$	0.1	CO
		235.0269		$C_{11}H_8O_2N_2Cl$	0.1	17	224.0110	$C_{10}H_7O_3NCl$	0.4	HCN , addition of ½ O_2
							206.0004	$C_{10}H_5O_2NCl$	0.3	HCN , H_2O, addition of ½ O_2
							196.0160	$C_9H_7O_2NCl$	-0.1	HCN , CO, addition of ½ O_2
							178.0054	C_9H_5ONCl	-0.3	HCN , CO, H_2O, addition of ½ O_2
			224.0109	$C_{10}H_7O_3NCl$	-0.2	25	206.0003	$C_{10}H_5O_2NCl$	-0.2	H_2O
							196.0160	$C_9H_7O_2NCl$	-0.1	CO
							178.0054	C_9H_5ONCl	-0.3	H_2O, CO
			206.0003	$C_{10}H_5O_2NCl$	-0.2	20	224.0110	$C_{10}H_7O_3NCl$	0.4	addition of H_2O
							196.0160	$C_9H_7O_2NCl$	-0.1	H_2O
							178.0053	C_9H_5ONCl	-0.5	CO
							150.0104	C_8H_5NCl	-0.9	CO (2x)
3	224.0110			$C_{10}H_7O_3NCl$	0.4	40	206.0004	$C_{10}H_5O_2NCl$	0.5	H_2O
							196.0160	$C_9H_7O_2NCl$	-0.1	CO
							178.0054	C_9H_5ONCl	-0.3	H_2O, CO
		206.0004		$C_{10}H_5O_2NCl$	0.3	20	224.0110	$C_{10}H_7O_3NCl$	0.4	addition of H_2O
							196.0161	$C_9H_7O_2NCl$	0.6	H_2O
							178.0055	C_9H_5ONCl	0.5	CO
							150.0105	C_8H_5NCl	-0.1	CO (2x)
4	238.0265			$C_{11}H_9O_3NCl$	-0.1	16	224.0109	$C_{10}H_7O_3NCl$	0.1	CH_2
							206.0003	$C_{10}H_5O_2NCl$	0.0	CH_2, H_2O
							196.0160	$C_9H_7O_2NCl$	-0.1	CH_2, CO
							178.0053	C_9H_5ONCl	-0.6	CH_2, CO, H_2O
		224.0108		$C_{10}H_7O_3NCl$	-0.4	40	206.0003	$C_{10}H_5O_2NCl$	-0.2	H_2O
							196.0159	$C_9H_7O_2NCl$	-0.5	CO
							178.0053	C_9H_5ONCl	-0.5	H_2O, CO
5	285.0582			$C_{12}H_6D_4O_4N_2Cl$	2.5	15	265.0350	$C_{12}H_6D_2O_3N_2Cl$		D_2O
							237.0400	$C_{11}H_6D_2O_2N_2Cl$	2.2	D_2O, CO
							227.0302	$C_{10}H_4D_3O_3NCl$	2.0	C_2H_2DNO
							225.0174	$C_{10}H_6DO_3NCl$	1.1	D_2O, CO, DCN, addition of ½ O_2
							207.0068	$C_{10}H_4DO_2NCl$	0.8	D_2O, H_2O, CO, DCN, addition of ½ O_2
		237.0400		$C_{11}H_6D_2O_2N_2Cl$	2.2	20	225.0175	$C_{10}H_6DO_3NCl$	1.5	DCN, addition of ½ O_2
							207.0068	$C_{10}H_4DO_2NCl$	0.8	DCN, H_2O, addition of ½ O_2
			225.0174	$C_{10}H_6DO_3NCl$	1.0	20	207.0067	$C_{10}H_4DO_2NCl$	0.7	H_2O
			207.0068	$C_{10}H_4DO_2NCl$	0.8	12	225.0174	$C_{10}H_6DO_3NCl$	1.0	addition of H_2O
							179.0118	C_9H_4DONCl	0.4	CO
							151.0167	C_8H_4DNCl	-0.3	CO (2x)

(+18 u, Table 1). The source of the added water molecule remained unclear, but the use of deuterium oxide and water-^{18}O as solvents for Compound **2** in offline-ESI-MS/MS experiments excluded the possibility that it originated from the solvation/ionization process. No shifts due to either ^{18}O- or D_2O-uptake

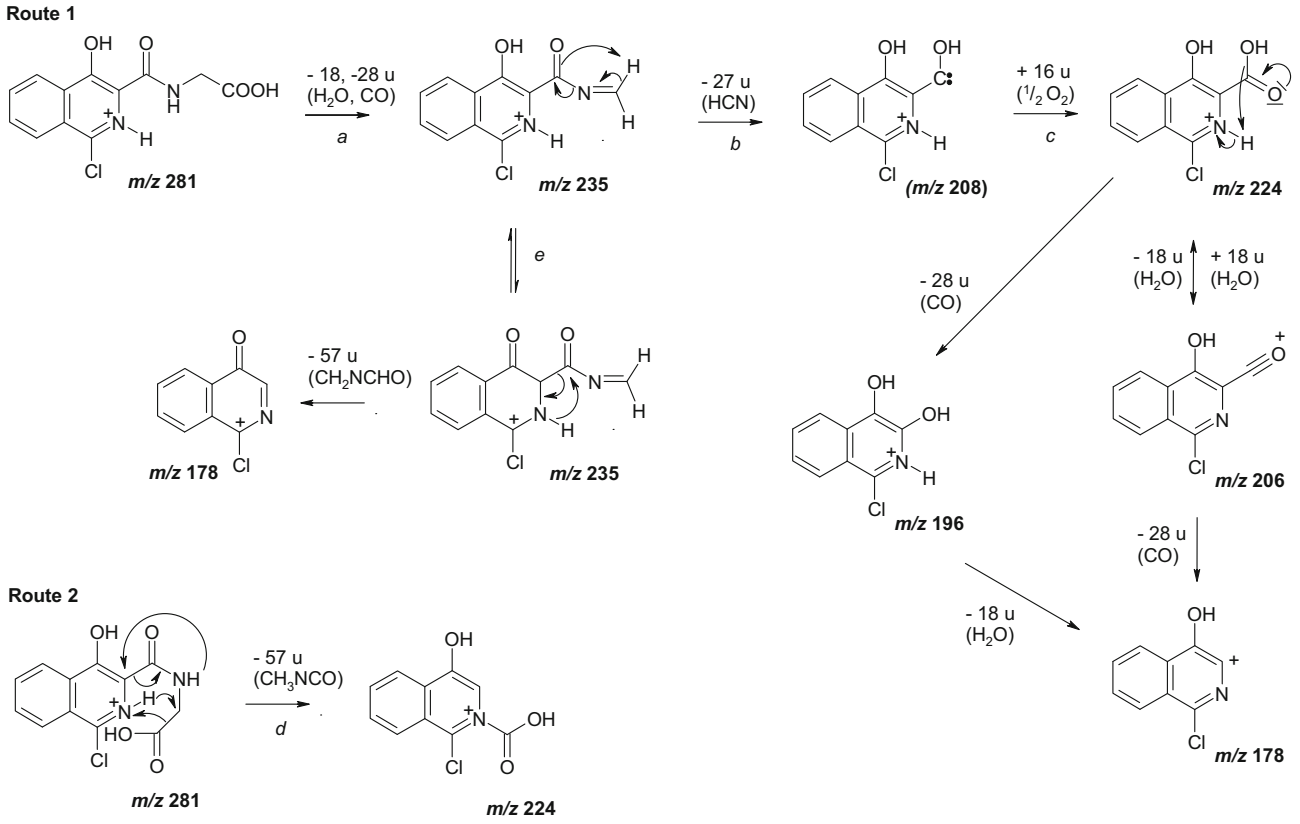

Scheme 2. Proposed dissociation pathway of Compound **2** [(1-chloro-4-hydroxy-isoquinoline-3-carbonyl)-amino]-acetic acid.

were observed for the regenerated ion at *m/z* 224 (data not shown). The efficiency of restoration was surprisingly high, which allowed to conduct "ping-pong" MS/MS experiments between *m/z* 224 and *m/z* 206. The product ion at *m/z* 224 was dissociated to *m/z* 206 at a normalized collision energy of 25 (arbitrary units), and the subsequent isolation and storage of *m/z* 206 (normalized collision energy set to 5 arbitrary units) yielded *m/z* 224 in high amounts that enabled MS^7 experiments going forth and back between the two precursor-/product ions.

Conclusions

The mass spectrometric behavior of selected substituted isoquinolines, which possess great potential for clinical utility as prolylhydroxylase inhibitors, was studied, and unusual dissociation pathways were observed using in-time and in-space tandem mass spectrometry. The formation of a particularly favored 3-carboxylic acid structure was suggested based on various MS experiments and analyses of synthetically derived compounds comprising solid-phase structures of assumed gas phase-derived product ions. Detailed mechanistic studies employing for instance density functional theory (DFT) calculation as well as measurements of additional structurally related substances might clarify which factors are essential for the observed phenomena and allow the identification of the major driving force.

Acknowledgments

The authors acknowledge support of this study from the Manfred Donike Institute for Doping Analysis, Cologne, Germany.

References

1. Pihlajaniemi, T.; Myllyla, R., Kivirikko, K. I. Prolyl 4-Hydroxylase and Its Role in Collagen Synthesis. *J. Hepatol.* **1991**, *13*(*Supp 3*), S2–S7.
2. Kivirikko, K. I.; Helaakoski, T.; Tasanen, K.; Vuori, K.; Myllyla, R.; Parkkonen, T.; Pihlajaniemi, T. Molecular Biology of Prolyl 4-Hydroxylase. *Ann. N.Y. Acad. Sci.* **1990**, *580*, 132–142.
3. Prockop, D. J.; Kivirikko, K. I. Collagens: Molecular Biology, Diseases, and Potentials for Therapy. *Annu. Rev. Biochem.* **1995**, *64*, 403–434.
4. Hirsilä, M.; Koivunen, P.; Günzler, V.; Kivirikko, K.; Myllyharju, J. Characterization of the Human Prolyl 4-Hydroxylases that Modify the Hypoxia-Inducible Factor. *J. Biol. Chem.* **2003**, *278*, 30772–30780.
5. Epstein, A. C.; Gleadle, J. M.; McNeill, L. A.; Hewitson, K. S.; O'Rourke, J.; Mole, D. R.; Mukherji, M.; Metzen, E.; Wilson, M. I.; Dhanda, A.; Tian, Y. M.; Masson, N.; Hamilton, D. L.; Jaakkola, P.; Barstead, R.; Hodgkin, J.; Maxwell, P. H.; Pugh, C. W.; Schofield, C. J.; Ratcliffe, P. J. *C. elegans* EGL-9 and Mammalian Homologs Define a Family of Dioxygenases that Regulate HIF by Prolyl hydroxylation. *Cell* **2001**, *107*, 43–54.
6. Bruick, R. K.; McKnight, S. L. A Conserved Family of Prolyl-4-Hydroxylases that Modify HIF. *Science* **2001**, *294*, 1337–1340.
7. Jaakkola, P.; Mole, D. R.; Tian, Y. M.; Wilson, M. I.; Gielbert, J.; Gaskell, S. J.; Kriegsheim, A.; Hebestreit, H. F.; Mukherji, M.; Schofield, C. J.; Maxwell, P. H.; Pugh, C. W.; Ratcliffe, P. J. Targeting of HIF-α to the von Hippel-Lindau ubiquitilation complex by O2-regulated prolyl hydroxylation. *Science* **2001**, *292*, 468–472.
8. Ivan, M.; Kondo, K.; Yang, H.; Kim, W.; Valiando, J.; Ohh, M.; Salic, A.; Asara, J. M.; Lane, W. S.; Kaelin, W. G., Jr. HIFα Targeted for VHL-Mediated Destruction by Proline Hydroxylation: Implications for O2 Sensing. *Science* **2001**, *292*, 464–468.
9. Yu, F.; White, S. B.; Zhao, Q.; Lee, F. S. HIF-1α Binding to VHL is Regulated by Stimulus-Sensitive Proline Hydroxylation. *Proc. Natl. Acad. Sci. U.S.A.* **2001**, *98*, 9630–9635.
10. Safran, M.; Kaelin, W. G., Jr. HIF Hydroxylation and the Mammalian Oxygen-Sensing Pathway. *J. Clin. Invest.* **2003**, *111*, 779–783.
11. Metzen, E.; Ratcliffe, P. HIF Hydroxylation and Cellular Oxygen Sensing. *Biol. Chem.* **2004**, *385*, 223–230.

12. Bruick, R. Oxygen Sensing in the Hypoxic Response Pathway: Regulation of the Hypoxia-Inducible Transcription Factor. *Genes Dev.* **2003**, *17*, 2614–2623.
13. Warnecke, C.; Griethe, W.; Weidemann, A.; Jurgensen, J.; Willam, C.; Bachmann, S.; Ivashchenko, Y.; Wagner, I.; Frei, U.; Wiesener, M.; Eckardt, K. Activation of the Hypoxia-Inducible Factor Pathway and Stimulation of Angiogenesis by Application of Prolyl Hydroxylase Inhibitors. *FASEB J.* **2003**, *17*, 1186–1188.
14. Bruick, R. K.; McKnight, S. L. Building Better Vasculature. *Genes Dev.* **2001**, *15*, 2497–2502.
15. Jelkmann, W. Molecular Biology of Erythropoietin. *Intern. Med.* **2004**, *43*, 649–659.
16. Ratcliffe, P. From Erythropoietin to Oxygen: Hypoxia-Inducible Factor Hydroxylases and the Hypoxia Signal Pathway. *Blood Purif.* **2002**, *20*, 445–450.
17. del Peso, L.; Castellanos, M.; Temes, E.; Martin-Puig, S.; Cuevas, Y.; Olmos, G.; Landazuri, M. The von Hippel Lindau/Hypoxia-Inducible Factor (HIF) Pathway Regulates the Transcription of the HIF-Proline Hydroxylase Genes in Response to Low Oxygen. *J. Biol. Chem.* **2003**, *278*, 48690–48695.
18. Nietfeld, J.; de Jong, L.; Kemp, A.The Influence of 2-Oxoglutarate on the Activity of Prolyl 4-Hydroxylase. *Biochim. Biophys. Acta*. **1982**, *704*, 321–325.
19. Mole, D.; Schlemminger, I.; McNeill, L.; Hewitson, K.; Pugh, C.; Ratcliffe, P.; Schofield, C. 2-Oxoglutarate Analogue Inhibitors of HIF Prolyl Hydroxylase. *Bioorg. Med. Chem. Lett.* **2003**, *13*, 2677–2680.
20. Cunliffe, C.; Franklin, T. Inhibition of Prolyl 4-Hydroxylase by Hydroxyanthraquinones. *Biochem. J.* **1986**, *239*, 311–315.
21. Dowell, R.; Hadley, E. Novel Inhibitors of Prolyl 4-Hydroxylase. *J. Med. Chem.* **1992**, *35*, 800–804.
22. Wang, J.; Buss, J.; Chen, G.; Ponka, P.; Pantopoulos, K. The Prolyl 4-Hydroxylase Inhibitor Ethyl-3,4-Dihydroxybenzoate Generates Effective Iron Deficiency in Cultured Cells. *FEBS Lett.* **2002**, *529*, 309–312.
23. Warshakoon, N. C.; Wu, S.; Boyer, A.; Kawamoto, R.; Sheville, J.; Renock, S.; Xu, K.; Pokross, M.; Zhou, S.; Winter, C.; Walter, R.; Mekel, M.; Evdokimov, A. G. Structure-Based Design, Synthesis, and SAR Evaluation of a New Series of 8-Hydroxyquinolines as HIF-1α Prolyl Hydroxylase Inhibitors. *Bioorg. Med. Chem. Lett.* **2006**, *16*, 5517–5522.
24. Warshakoon, N. C.; Wu, S.; Boyer, A.; Kawamoto, R.; Renock, S.; Xu, K.; Pokross, M.; Evdokimov, A. G.; Zhou, S.; Winter, C.; Walter, R.; Mekel, M. Design and Synthesis of a Series of Novel Pyrazolopyridines as HIF-1α Prolyl Hydroxylase Inhibitors. *Bioorg. Med. Chem. Lett.* **2006**, *16*, 5687–5690.
25. Tucker, H.; Thomas, D. Novel Inhibitors of Prolyl 4-Hydroxylase. 2. 5-Amide Substituted pyridine-2-carboxylic acids. *J. Med. Chem.* **1992**, *35*, 804–807.
26. Hales, N.; Beattie, J. Novel Inhibitors of Prolyl 4-Hydroxylase. 5. The Intriguing Structure-Activity Relationships Seen with 2,2′-Bipyridine and Its 5,5′-Dicarboxylic Acid Derivatives. *J. Med. Chem.* **1993**, *36*, 3853–3858.
27. Cunliffe, C.; Franklin, T.; Hales, N.; Hill, G. Novel Inhibitors of Prolyl 4-Hydroxylase. 3. Inhibition by the Substrate Analogue N-Oxaloglycine and Its Derivatives. *J. Med. Chem.* **1992**, *35*, 2652–2658.
28. Baader, E.; Tschank, G.; Baringhaus, K.; Burghard, H.; Gunzler, V. Inhibition of Prolyl 4-Hydroxylase by Oxalyl Amino Acid Derivatives in Vitro, in Isolated Microsomes and in Embryonic Chicken Tissues. *Biochem. J.* **1994**, *300*, 525–530.
29. Fibrogen Inc. Development Pipeline. 2007, http://www.fibrogen.com/pipeline/chart/anemia.html#mid (accessed 09-20-2007).
30. Wang, Q.; Gou, G.; Guenzler, V.; Neff, T.; Klaus, S.; Turtle, E.; Molineaux, C.; Yeowell, D., Lin, A. Stimulation of Erythropoiesis and Treatment of Anemia in Rodents by Oral Administration of FG-2216, a Novel HIF-Prolyl Hydroxylase Inhibitor. *J. Am. Soc. Nephrol.* **2004**, *15*, 773A.
31. Hsieh, M. M.; Linde, N. S.; Wynter, A.; Metzger, M.; Wong, C.; Langsetmo, I.; Lin, A.; Smith, R.; Rodgers, G. P.; Donahue, R. E.; Klaus, S. J.; Tisdale, J. F. HIF Prolyl Hydroxylase Inhibition Results in Endogenous Erythropoietin Induction, Erythrocytosis, and Modest Fetal Hemoglobin Expression in Rhesus Macaques. *Blood* **2007**, *110*, 2140–2147.
32. Suzuki, M.; Nunami, K.; Matsumoto, K.; Yoneda, N.; Miyoshi, M. A Facile Synthesis of 1-Oxo-1,2-Dihydroxyisoquinoline-3-Carboxylate and 2-Pyridone-6-Carboxylate Derivatives. *Synthesis* **1978**, 461–462.
33. Fibrogen. EP 1 538 160 A1, European Patent Office: 2005.